Band-Theoretic Study of the Metallic Character of the Alkali–Noble Metal Alloys*

T. L. LIU, H. AMAR

Department of Physics, Temple University, Philadelphia, Pennsylvania

The electronic band structures of CsAu and LiAg have been determined by a combination of the Green's function (KKR) and the quantum-defect (QDM) methods. The construction of the phase shifts is based on the preliminary determination of the appropriate quantum defects. The latter are adjusted to take into account an estimated charge transfer of 0.55e from alkali to the noble metal. Our results show that despite the similarily of their constituents and of their crystal structures the two alloys exhibit markedly different features: CsAu is an extrinsic n-type semiconductor with a 2.7-eV minimum gap in the (111) direction, while LiAg has the band structure of a metallic alloy, with the (cubic) Brillouin zone full except for small empty regions at the corners. Our results for CsAu are in agreement with available data and with one previous calculation. For LiAg, there are no experimental data available for comparison.

INTRODUCTION

The metal–semimetal transitions have been and are being extensively studied in metallic oxides and semiconducting compounds. Our work on the band structure of binary metallic alloys of the Cu–Zn [1] family has led us to investigate the evolution of the metallic character in the noble metal–alkali family of alloys. We chose as prototypes CsAu and LiAg. The first alloy has been the object of extensive experimental work. Reitz and Wood[2] have calculated its band structure at point Γ and two end points of the Brillouin zone. On the other hand, very little (if any) work has been done on the second alloy. We hope that our results will stimulate such work.

The method used is the highly convergent KKR (or Green's function) method in combination with the quantum-defect method (QDM). The essentials of the method are first described in Sec. I. We summarize in Sec. II some of the significant properties of the two alloys and of their metallic constituents. The actual calculation and the results are described in Sec. III. Section IV contains a discussion of these results.

I. THE COMBINED KKR-OD METHOD

Korringa[3] and Kohn–Rostoker's[4] papers contain the fundamentals of the KKR's method, while Ham and Segall's[5] calculations describe fully its application to simple metals. We discussed in other publications its extension to ordered alloys. Here we shall simply review the basic results in the form in which we have used them. The Schrödinger equation (with the exact boundary conditions) is transformed into an integral equation by means of the corresponding Green's function. The integral equation is shown to be derivable from a variation principle. The crystal potential is assumed to be of the muffin-tin type, i.e., spherically symmetric within each cell as follows: $V=V(r)$, $r<r_m$, and $V=$constant, $r\geq r_m$. This approximation allows the following expansion of the crystal wave function

$$\Psi_{\alpha_j}(\mathbf{k}_{\alpha j},\ \mathbf{r}_j)=\sum_{l}^{l\max}\sum_{\gamma} i^l C_{l\gamma}{}^{\alpha} i R_l{}^{(j)}(r_j) K_{l\gamma}{}^{\alpha j}(\mathbf{r}_j), \quad (1)$$

where $K_{l\gamma}{}^{\alpha}$ are the Kubic harmonics belonging to the irreducible representation α_j and $R_l(r)$ satisfies the differential equation

$$\left[-\frac{1}{r^2}\frac{d}{dr}\left(r^2\frac{d}{dr}\right)+\frac{l(l+1)}{r^2}+V(r)-E\right]R_l(r)=0. \quad (2)$$

The determination of the constants in (1) (via the variational principle) leads to a linear homogeneous system whose secular determinant is given by

$$0=\det\{B_{l\gamma,l'\gamma'}{}^{jj'}(E,\mathbf{k})+\kappa\delta_{ll'}\delta_{jj'}\delta_{\gamma\gamma'}\cot\delta_l{}^{(j)}\}, \quad (3)$$

where $B_{l\gamma,l'\gamma'}{}^{jj'}$ are the structure constants and

$$\kappa=+(E)^{1/2} \qquad E>0$$
$$=i(-E)^{1/2} \qquad E<0.$$

For each $\mathbf{k}$ point, and each value of the energy the "structural" part B of the basic determinantal equation (3) depends only on the crystal structure and lattice distance. The phase shift is given by

$$\cot\delta_l{}^{(j)}=(\eta_l'-\eta_l L_l{}^{(j)})/(j_l'-j_l L_l{}^{(j)})\mid_{r_j=R_m}, \quad (4)$$

where

$$L_l{}^{(j)}(r_j)=[R_l{}^{(j)}(r_j)]^{-1}(d/dr_j)R_l{}^{(j)}(r_j) \quad (5)$$

are the logarithmic derivatives and $j_l(\kappa r)$ and $\eta_l(\kappa r)$ are the standard spherical Bessel functions.

* Work supported by the U.S. Atomic Energy Commission.

[1] K. H. Johnson and H. Amar, Phys. Rev. **139**, A760 (1965); H. Amar, K. H. Johnson, and K. P. Wang, *ibid.* **149**, 672 (1966).

[2] J. R. Reitz and V. E. Wood, J. Phys. Chem. Solids **23**, 229 (1962).

[3] J. Korringa, Physica **13**, 392 (1947).

[4] W. Kohn and N. Rostoker, Phys. Rev. **94**, 1111 (1954).

[5] F. S. Ham, and B. Segall, Phys. Rev. **124**, 1786 (1961).

The determination of the phase shifts is usually done in the following steps: (a) Construction of a crystal potential, (b) numerical solution of the differential equation (2), and (c) determination of $\cot\delta_l$ using (4) and (5).

The QD method allows the determination of the phase shifts from the observed spectroscopic data of the free atom. The construction of a potential, and all related approximations are thus avoided. This method, initiated by Kuhn and Van Vleck[6] was substantially improved by Brooks and Ham[7–9] whose procedure we follow. The method may be summarized as follows. The potential felt by a valence electron in a monovalent atom of nuclear charge Z may be approximated by

$$V(r)=-(2Z/r)+g(r) \qquad 0<r<r_1 \qquad (6a)$$

$$=-2/r \qquad r>r_m, \qquad (6b)$$

and is piecewise continuous in narrow range $r_1\leq r\leq r_m$. Here $g(r)$ is a continuous function. The wave function may be expanded

$$\Psi(r)=\sum A_{lm}Y_{lm}(\theta,\phi)R_l(r), \qquad R_l=U_l/r, \quad (7)$$

and $U_l(r)$ satisfies the differential equation

$$[d^2U^l(r,E)/dr^2]$$

$$+\{E-V(r)-[l(l+1)/r^2]\}U^l(rE)=0. \quad (8)$$

The energy may be written $E=-1/n^2$, where $n=\mathfrak{n}$ is an integer in the hydrogen atom, and $n=\mathfrak{n}-\delta(n)$ in the alkalis and other atoms. Thus in general $n=n(E)$ is a number that can be used to label the observed energy levels in the free atom. The essence of the QDM is to consider a continuous range of energies and to associate with each value E, a number $n(E)$ and the associated quantum defect $\delta(n)=\delta(E)=\mathfrak{n}-n(E)$, where $\mathfrak{n}$ is an integer. A thorough study by Ham[7,10] of the Coulomb wave functions [solutions of (8)], and of the empirical spectroscopic data[11] led to a prescription allowing the determination (by interpolation and extrapolation) of the quantum defects. Ham showed that the general solution of (8) may be written

$$U^l(r,E)=\alpha(n)^0U^{ln}(r)+\gamma(n)^2U^{l,n}(r), \qquad (9)$$

where ${}^0U(0)=0$ and ${}^2U$ is singular at the origin. These functions are known and have been tabulated[10,12] and the ratio of their coefficients is related to the quantum defect by the equation

$$\alpha(n)/\gamma(n)=-[\Gamma(n+l+1)/n^{2l+1}\Gamma(n-l)\tan\pi\delta(n)]$$

$$=-[\tan\pi\eta(n)]^{-1}, \qquad (10)$$

where Γ is the usual gamma function, and η or eta defect is a related quantum defect whose smooth behavior allows better interpolations.

Once the quantum defect $\delta(E)$ [or the eta defect $\eta(E)$] has been constructed, the function $U^l(r)$ is constructed from the tables, and the logarithmic derivative of $U^l(r)$ may be calculated at the muffin-tin radius r_m. This leads to the determination of the phase shifts and of $\cot\delta_l$ in the determinantal equation (3).

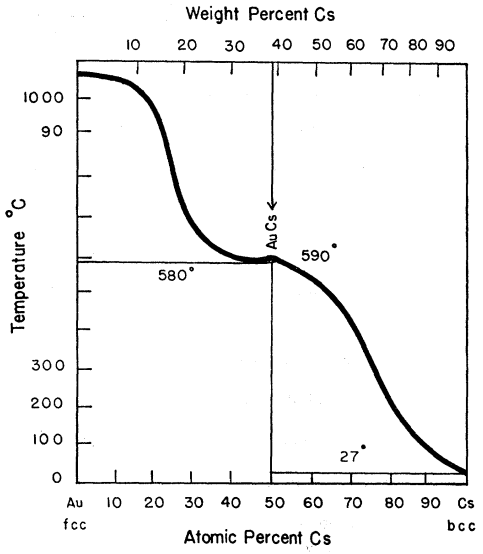

FIG. 1. Phase diagram of the Au–Cs system (Elliott).

II. PHYSICAL PROPERTIES

It is appropriate at this stage to describe the relevant physical properties of the alloys under study and of their simple constituents. Table I summarizes the free-atom and bulk properties of the alkalis Cs and Li and of the noble metals Au and Ag. Note among these properties the respective values of the resistivity, of the electronegativity, and the radii of the free atom and ion of each element. The similarity of the electronic configurations and of the crystal structures, suggests a great similarity in the properties of the corresponding alloys.

Tables II and III contain a summary of the properties of the alloys CsAu and LiAg. Indeed they have the same cesium chloride structure, despite the unfavorable alloying size factor in CsAu. Beyond that, some appreciable differences appear between the two alloys. CsAu exhibits a stronger volume contraction and a

[6] T. S. Kuhn and J. H. Van Vleck, Phys. Rev. **79**, 382 (1950).
[7] F. S. Ham, Solid State Phys. **1**, 127 (1955).
[8] H. Brooks and F. S. Ham. Phys. Rev. **112**, 344 (1958).
[9] H. Brooks, Nuovo Cimento Suppl. **7**, 165 (1958).
[10] F. S. Ham, "Tables for the Calculation of Coulomb Wave Functions," Technical Report No. 204, Cruft Laboratory, Harvard University, Cambridge, Mass., 1955 (unpublished).
[11] C. E. Moore, Natl. Bur. Std. Circ. No. 467, Vols. 1 and 3.
[12] M. Blume, N. Briggs, and H. Brooks, "Tables of Coulomb Wave Functions," Technical Report No. 260, Cruft Laboratory, Harvard University, Cambridge, Mass., 1959 (unpublished).

TABLE I. Free atomic and simple metallic information.

	Cs	Au	Li	Ag
Atomic number	55	79	3	47
Configuration	$4d^{10}5s^25p^6$ $6s$	$4d^{10}4f^{14}5s^2$ $5p^65d^{10}6s$	$2s$	$4d^{10}5s$
Atomic radius	3.04 Å	1.59 Å	1.72 Å	1.59 Å
Ionic radius	1.65 Å(+)	1.37 Å(+) 1.49 Å(−)	0.78 Å(+)	1.13 Å(+) 1.49 Å(−)
R(ion)/R(atom)	0.629	0.951	0.513	0.784
Crystal structure	bcc	fcc	bcc	fcc
Lattice constant	6.079 Å	4.0786 Å	3.5089 Å	4.0862 Å
Atomic volume	69.19 cm³/m	10.22 cm³/m	13.02 cm³/m	10.27 cm³/m
Electronegativity:				
Pauling	0.7	2.1	1.0	1.7
Gordy and Thomas	0.76	2.30	0.95	1.80
Electric resistivity ($\mu\Omega$·cm)	19 (0°C)	2.97 (100°C)	8.55 (0°C)	1.468 (0°C)
Thermal conductivity (Ws/cm·°K)	0.61 (20°K)	3.1∼(273°K)	0.71 (273°K)	4.17 (273°K)

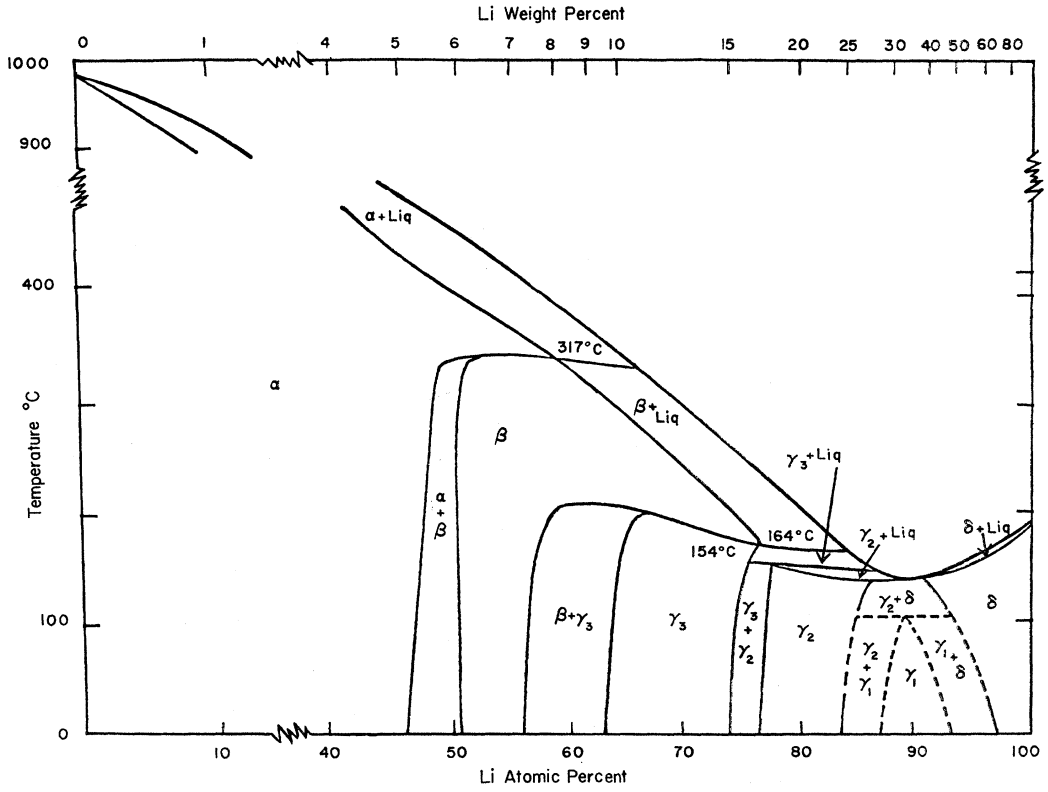

FIG. 2. Phase diagram of LiAg (Freeth and Raynor).

probably higher ionicity. The phase diagrams (Figs. 1 and 2) are markedly different. The diagram of LiAg [13] is similar to that of most metallic alloys, while in CsAu [14] there exists only one very narrow phase.

The optical properties of CsAu have been studied by Spicer *et al.*[15] The optical absorption compared to that of pure gold, shows a marked decrease at photoenergies below 2.5 eV and a rise above this value; and also shows three exciton peaks. This indicates that when gold is combined with cesium to form CsAu, a metal to semiconductor transition occurs. In the photoemission experiments they found that the photoemission in the spectral range around 2.2 eV is due principally to the excitation of electrons from a low-lying band which is identified with the valence band of a semiconductor. These results confirm the semiconducting properties of CsAu and predict the forbidden gap to be about 2.6 eV.

The resistivity of CsAu at temperatures between 4.2° and 410°K is 5000 times higher than that of pure gold ($\sim$0.01 $\Omega\cdot$cm).[15] The observed resistivity of CsAu decreases as the temperature increases at higher temperatures. The Hall coefficient is found to be negative (carrier concentration 10^{18}–10^{19} cm^{-3}).[15] Thus, all experimental information (resistivity and its temperature dependence, sign of Hall constant, etc.) points out that CsAu is an n-type semiconductor. Wooten *et al.*[16]

TABLE II. Alloy information (CsAu).

Crystal structure	CsCl type (see Fig. 10)
Lattice constant	4.263 Å
Equivalent-volume sphere radius	3.968 Å
Inscribed sphere radius	3.489 Å
Muffin-tin radius[a]	3.3800 Å (z=5.2)
Cs–Au distance	3.6917 Å
$R(-\text{ion})/R(+\text{ion})$	0.903<1.37
Size factor $R(\text{Cs}/R(\text{Au})$	1.8939 (unfavorable)
Volume contraction[a]	42%
Muffin-tin potential[a]	−0.5356 Ry
$4\pi^2/a^2$ (a=lattice constant)	0.6079
Electric resistivity	$\sim$0.01 $\Omega\cdot$cm
Amount of ionicity	
Pauling	51.4%
Sanderson	47.9%
Cohesion	52.9%
Density	7.065 g/cm^3

[a] Values used in this work.

[13] W. E. Freeth and G. V. Raynor, J. Inst. Metals **82**, 569 (1954).
[14] G. Kienast and J. Verma, Z. Anorg. Allgem. Chem. **310**, 143 (1961); R. P. Elliott, *Constitution of Binary Alloys, First Supplement* (McGraw-Hill Book Co., New York, 1965).
[15] W. E. Spicer, A. H. Sommer, and J. H. White, Phys. Rev. **115**, 57 (1959); W. E. Spicer, *ibid.* **125**, 1297 (1961).
[16] F. Wooten and G. A. Condas, Phys. Rev. **131**, 657 (1963).

TABLE III. Alloy information (LiAg).

Crystal structure	CsCl (see Fig. 10)
Lattice constant	3.169 Å
Equivalent-volume sphere radius	2.9441 Å
Inscribed sphere radius	2.5889 Å
Muffin-tin radius[a]	2.5313 Å (z=4.5)
Li–Ag distance	2.7390 Å
$R(-\text{ion})/R(+\text{ion})$	1.91>1.37
Size factor $R(\text{Li})/R(\text{Ag})$	1.0810 (favorable)
Volume contraction[a]	18.15%
Muffin-tin potential[a]	−0.7219 Ry
$4\pi^2/a^2$ (a=lattice constant)	1.1042
Amount of ionicity	
Pauling	18.3%
Sanderson	31.5%
Cohesion	50.4%
Density	5.990 g/cm^3

[a] Values used in this work.

measured the Seebeck coefficient of CsAu at 300°K, and using some reasonable assumptions (optical scattering predominant at 300°K) derived from it the location of the Fermi level, namely 0.021 eV (or about 0.0015 Ry) above the conduction band edge.

The phase diagram of LiAg has been established by Freeth and Raynor.[13] This is practically the only experimental work available on this compound. We have been unable to find any information on its other physical properties.

The large difference in the electrochemical properties of the constituents and the substantial volume contraction indicate that these alloys have some ionic character in their binding. We first tried the methods of Pauling[17] (essentially based on the electronegativity difference) and Sanderson[18] (based on stability ratio) to estimate the amount of ionicity. The amounts found were too low to allow cohesion. A calculation of the ionicity necessary to make cohesion possible led to the value of 53% for CsAu and 50% for LiAg. We settled on a common value of 55% for both compounds.

III. CALCULATION AND RESULTS

The spectroscopic tables[11] provide the standard quantum defects. Using Eq. (10), one can calculate the corresponding η defects. However the occurrence of ionicity requires a correction $\Delta\eta$ to these η defects. Brooks and Ham[8,9] have shown that whenever the potential outside the muffin-tin sphere departs from the expected Coulomb's potential (6b) by a small

[17] L. Pauling, *The Nature of the Chemical Bond* (Cornell University Press, Ithaca, N.Y., 1965), 3rd ed.
[18] R. T. Sanderson, *Chemical Periodicity* (Reinhold Publ. Corp., New York, 1966).

TABLE IV. Quantum defects (Cs and Au).

m	$-E$	δ_s	$-E$	η_p	$-E$	η_d
			Cs			
4					(1.1262)	0.3929
5					0.1535403	0.4829
6	0.2862062	0.1308	0.1809736	−0.3747	0.0801213	0.4771
7	0.1172939	0.0801	0.0867584	−0.4035	0.0487201	0.4745
8	0.0646063	0.0658	0.0514193	−0.4144	0.0327012	0.4721
9	0.0409719	0.0595	0.0340790	−0.4195	0.0234522	0.4707
10	0.0283086	0.0565	0.0242562	−0.4228	0.0176368	0.4696
			Au			
5	(8.4681)	−0.3436	(5.1)	0.2967	(4.4981)	0.4907
6	0.678908	−0.2144	0.3115664	0.2675	0.1130646	0.0523
7	0.1815754	−0.3468	0.1262601	0.2056	0.0630138	0.0227
8	0.0880998	−0.3692	0.0690393	0.2041	0.0402434	0.0185
9	0.0522123	−0.3763			0.0277032	−0.0111
10	0.0345625	−0.3792			0.0204302	0.0022

amount $\Delta V(r)$, a correction to the η defect can be estimated as follows:

$$\eta = -(2\sec^2\pi\eta)^{-1}\int_{R_m}^{R}\Delta V(r)[U_h^{l,n}(r)]^2dr,$$

where $U_h^{l,n}$ is the radial wave function when ΔV is negligible.

We list the standard quantum defects in Tables IV and V. Following the outlined procedures we calculate the corresponding η defects and the corrections $\Delta\eta$. In the latter calculation we assume a 55% ionicity, calculate the corresponding ΔV which takes into account the uniform distribution of the extra charge transferred to or from the atoms to make negative or

TABLE V. Quantum defects (Li and Ag).

m	$-E$	δ_s	$-E$	η_p	$-E$	η_d
			Li			
2	0.396294	0.4115	0.2604768	0.0547		
3	0.148368	0.4039	0.1144745	0.0500	0.1112146	0.0031
4	0.077233	0.4016	0.0639511	0.0486	0.0625491	0.0021
5	0.047275	0.4009	0.0407495	0.0481	0.0400261	0.0018
6	0.031891	0.4003	0.0282167	0.0483	0.0277932	0.0018
7	0.022958	0.4003	0.0206848	0.0478	0.0204192	0.0018
8	0.017315	0.4001	0.0158160	0.0491	0.0156367	0.0027
			Ag			
4	(7.7068)	−0.3602	(4.8368)	0.3400	(4.8368)	0.156
5	0.5568574	−0.3401	0.2819591	0.1564	0.1125477	0.0392
6	0.1690475	−0.4321	0.1154926	0.0648	0.0628525	0.0159
7	0.0840166	−0.4499	0.0639003	0.0470	0.0401266	0.0099
8	0.0503507	−0.4565	0.0406364	0.0408	0.0278346	0.0072
9	0.0335481	−0.4597	0.0281289	0.0388	0.0204378	0.0056

positive ions. These corrected η defects are used in the determination of the radial wave functions, and their logarithmic derivatives at the muffin-tin radius.

The charge transfer implies a corresponding Madelung correction $M=-2\alpha\rho^2/r_{AB}$. Here α is the Madelung coefficient, ρ is the ionicity, and r_{AB} is the internuclear distance. To each electronic energy value E, there corresponds two values $E_{Cs}=E+M$ in the Cs or Li cell and $E_{Au}=E-M$ in the Au or Ag cell. The η defects and phase shifts corresponding to E_{Cs} and E_{Au} are calculated according to the prescription described above. If $\rho=0.55$, the Madelung corrections in CsAu and LiAg

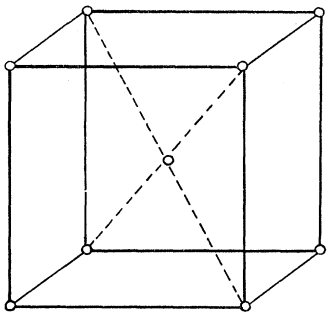

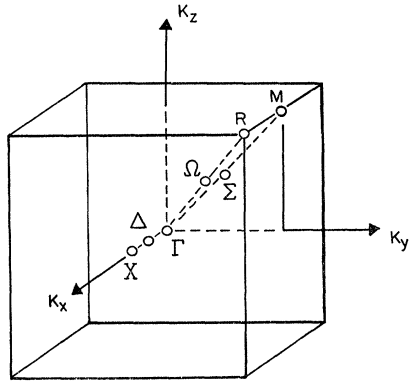

FIG. 3. CsCl Structure and the Brillouin zone.

are found to be -0.1528 and -0.2059 Ry, respectively. The muffin-tin potential is determined by averaging the Coulomb potential in the region between the muffin-tin sphere and the cell boundary (-0.5356 Ry for CsAu and -0.7219 Ry for LiAg). The structure constants of CsCl lattice (Fig. 3) are available from previous work and the evaluation of the secular determinants gives the energy eigenvalues (shown in Tables VI and VII). The bands are determined in the three principal directions (100), (110), and (111) of the Brillouin zone. Besides the end points and, Γ, the energy at the midpoint in each direction has been calculated. The states at the end points (e.g., R_{15}–$R_{25'}$, $X_{4'}$–X_1 etc.) are so labeled that the first letter refers to the character of the state in the alkali atom and the second refers to the noble metal atom. The band profiles of the two alloys are shown in Figs. 4 and 5. There is a definite contrast between the two.

TABLE VI. Energy eigenvalues of CsAu.

State	Energy (Ry) (zero at -0.5356 Ry)
$\Gamma_1(s)$	-0.352
$\Gamma_{15}(p)$	0.257
$\Gamma_{12}(d)$	0.287
$\Gamma_{25'}(d')$	0.452
$X_{4'}$–$X_1(p-s)$	-0.250
X_1–$X_{4'}(s-p)$	0.101
X_2–$X_{3'}(d'-f)$	0.140
M_3–$M_1(d-s)$	-0.255
M_3–$M_1(d-s)$	0.109
$M_{5'}$–$M_{5'}(p'-p')$	0.111
M_1–$M_3(s-d)$	0.224
$R_{2'}$–$R_1(f-s)$	-0.159
$R_{25'}$–$R_{15}(d'-p)$	0.039
R_{12}–$R_{12'}(d-h)$	0.143
R_{15}–$R_{25'}(p-d')$	0.347

TABLE VII. Energy eigenvalues of LiAg.

State	Energy (Ry) 0 = -0.7219	State	Energy (Ry) 0 = -0.7219
$\Gamma_1(s)$	-0.813	M_3–$M_1(d-s)$	-0.459
$\Gamma_{25'}(d')$	-0.455	M_1–$M_3(s-d)$	-0.452
$\Gamma_{12}(d)$	-0.449	M_5–$M_5(d''-d'')$	-0.437
$\Gamma_{15}(p)$	0.736	M_4–$M_2(g-d')$	-0.414
$\Gamma_{12}(d)$	0.964	M_3–$M_1(d-s)$	0.186
$\Gamma_{25'}(d')$	1.018	$M_{5'}$–$M_{5'}(p'-p')$	0.267
$X_{2'}$–$X_3(f'-d)$	-0.476	$R_{12'}$–$R_{12}(h-d)$	-0.469
$X_{3'}$–$X_2(f-d')$	-0.472	R_{15}–$R_{25'}(p-d')$	-0.439
$X_{4'}$–$X_1(p-s)$	-0.459	$R_{25'}$–$R_{15}(d'-p)$	0.511
$X_{5'}$–$X_5(p'-d'')$	-0.434	$R_{2'}$–$R_1(f-s)$	0.592
$X_{4'}$–$X_1(p-s)$	-0.167	R_1–$R_{2'}(s-f)$	0.596
X_1–$X_{4'}(s-p)$	0.168	R_{15}–$R_{25'}(p-d')$	0.663

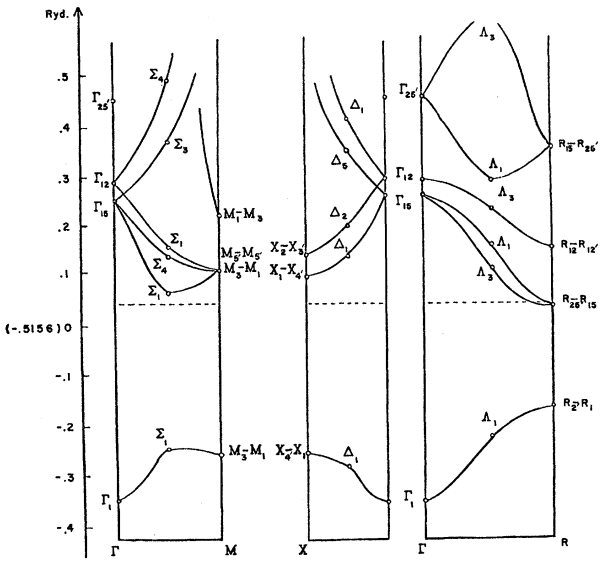

FIG. 4. Calculated bands of CsAu.

The bands of LiAg are very similar to those of other metallic alloys (such as CdAg etc.). There seems to be no forbidden band, although the bands in the (100) and (111) directions are separated into two groups. The Fermi level has been calculated by Houston's approximation method[19,20] and is shown in the diagram by a dotted line. The metallic character of this alloy is more obviously shown by the way the Fermi level cuts the bands. The unfilled part of the band in (111) direction leaves a "hole" near the point R in the first Brillouin zone, while in the other two directions, the lower bands are completely filled. A group of narrow d bands appears in the lower portion of the LiAg bands, which seems to come from the d bands of Ag.

On the other hand, the CsAu bands are typically of the semiconductor type, with a wide forbidden gap of 0.198 Ry (~2.7 eV) at the end of the (111) direction. The highest point of the valence band is at R_2–R_1 which is a state of predominantly s like character in the negatively ionized Au cell and f like character in Cs. The lowest point in the conduction band if $R_{25'}$–R_{15} which is d like in Cs and p like in Au. These results differ from those obtained by Reitz and Wood.[2] In their work, the highest point of the valence band is at R_1–R_2 and the lowest point of the conduction band is R_{15}–$R_{25'}$. Inspection of the band structure of other ionic compounds[21] shows that the lower state in the gap has a low l value that can be related to the negative ion. This is confirmed in our results. The band in the present work (100) and (111) directions are closer in shape to those of Reitz and Wood. Obviously the Fermi level could not be determined by the Houston method as in LiAg. Here we refer to the important paper by Wooten and Condas,[16] who extracted from the measurement of Seebeck coefficient the location of the Fermi level at 0.021 eV above the conduction band edge. A dotted line is also drawn in the CsAu diagram to indicate the value they obtained. Narrow d bands are not shown in the bands of CsAu although they are present in the bands of metallic Au.[22] The disappearance of the low-lying narrow d bands may give another example of the change in properties produced when Cs and Au combine to form a compound. On the other hand, in LiAg alloying does not seem to destroy the metallic behavior of the constituents.

IV. DISCUSSION AND CONCLUSION

Our work clearly shows that despite the similarity of their constituents and of their crystal structure, the alkali–noble metal alloys may have appreciably different physical properties. More specifically the metallic character of the constituents seems to survive the alloying process when the elemental constituents are light, and to vanish progressively as the alkali constituents become heavier.

In view of the identity of the crystal structures, the structural term B of the determinant of Eq. (3) plays little role in this trend. The difference in metallic be-

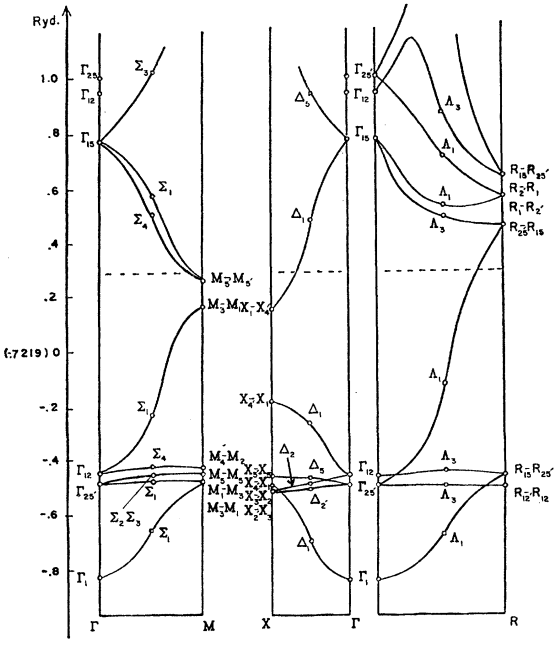

FIG. 5. Calculated bands of LiAg.

[19] W. V. Houston, Rev. Mod. Phys. **20,** 161 (1948).
[20] D. D. Betts, A. B. Bhatia, and M. Wyman, Phys. Rev. **104,** 37 (1956).
[21] D. H. Ewing and F. Seitz, Phys. Rev. **50,** 760 (1936).
[22] C. B. Sommers and H. Amar, Bull. Am. Phys. Soc. **13,** 57 (1968).

havior must be attributed to the phase-shift part of Eq. (3), itself immediately dependent on the quantum defects, hence on the particular atoms. Inspection of Tables I, II, and III suggests several possible determining factors such as atomic and relative ionic sizes, electronegativity, etc. Further theoretical and experimental work is needed before attempting a systematic interpretation.

ACKNOWLEDGMENTS

Part of this work was performed while the senior author (H. Amar) was a visiting professor at the University of Grenoble. H. Amar wishes to express his appreciation to Professor L. Néel, Professor R. Pauthenet, and his other Grenoble colleagues for courtesies extended during his stay in France. Dr. Reitz and Dr. Wood[2] are to be thanked for information and data sent during the performance of this work.

Discussion of Liu and Amar's Paper

H. Brooks (Harvard University): I don't think I quite followed how you handled the ionicity. It seems to me off-hand that if there is appreciable ionicity, the Madelung potential will have an appreciable variation over the cell so that the ordinary quantum defect approach which involves the assumption that the potential is strictly the ionic potential within the cell would run into difficulties.

H. Amar: We took into account the Madelung correction simply as a constant in each cell outside of the characteristic sphere. We made the standard constant correction.

H. Brooks: That is you took the value of the Madelung potential at the center of the cell and you extended it out, but then how did you jump to the next cell?

H. Amar: It has simply shifted the energies in the two cells.

H. Brooks: I see, so there's a discontinuity in the potential, a step in the potential, as you move from the cesium cell to the gold cell.

H. Amar: Yes.

W. Kohn (University of California, San Diego): May I ask a question about the choice of the phase shifts. You took those from atomic data?

H. Amar: Yes.

W. Kohn: Wouldn't you expect a possibly substantial modification due to the charge transfer that takes place?

H. Amar: The assumption of ionicity leads to the following two corrections: (a) A correction $\Delta\eta$ in the eta defect according to the prescription of Brooks and Ham: namely the extra charges on the gold and cesium sites create small changes δV in the central potentials leading to corrections $\Delta\eta$ described by Eq. (11). (b) A shift in the energies and potentials corresponding to the Madelung constant obtained by assuming that the displaced charges are point charges located at the nuclear sites. As stated before, no relativistic wave functions nor relativistic atomic potential were available for gold at the time we started this work, and the quantum-defect method seemed the best substitute for a good potential. A few months ago we received the required relativistic wave functions and we have recently completed a calculation of the relativistic band structure of gold.

W. Kohn: I have another question and I probably misunderstood something quite simple. We have here two valence electrons per unit cell, I guess, so it seems to me if you have a certain number of electrons present, you must have an equal number of holes. Your diagram didn't seem to show that and I am puzzled by it.

H. Amar: I imagine you refer to the dotted line indicating the possible location of the Fermi level. This is simply the Fermi level suggested by Wooten *et al.*, and based on the experimental determination of the Seebeck coefficient of impure CsAu.

W. Kohn: No, I'm just speaking in terms of counting electrons. It seems to me that either you just have a plain insulator, no holes and no electrons, or you have an equal number of holes and electrons.

H. Amar: You're quite right and strictly speaking this should lead to a Fermi level midway between the top of the valence band and the bottom of the conduction band.